

Electro-chemical reduction of MOX in LiCl

Masaki Kurata^{a,*}, Tadashi Inoue^a, Jerome Serp^b,
Michel Ougier^b, Jean-Paul Glatz^b

^a Central Research Institute of Electric Power Industry, Iwadokita 2-11-1, Komae-shi, Tokyo 201-8511, Japan

^b Institute for Transuranium element, Postfach 2340, D76125 Karlsruhe, Germany

Received 1 December 2003; accepted 8 March 2004

Abstract

Unirradiated MOX fuel particles with a few millimeters in size were reduced to a U–Pu alloy by electro-chemical means. The reaction started at the grain-boundary and formed metallic coral-like frames. The Pu-concentration in the alloy was measured to be lower than that in the original MOX. Pu-spots were observed in regions that were originally at the site of MOX-agglomerates. These facts indicated that U was reduced prior to Pu during electro-chemical reduction.

© 2004 Elsevier B.V. All rights reserved.

PACS: 82.45; 65.50

1. Introduction

The Central Research Institute of Electric Power Industry (CRIEPI) has been developing a technology for recycling nuclear spent fuels, which is based on the combination of pyrometallurgical reprocessing and metallic fuel fast reactor [1]. For treating spent oxide fuels with this technology, a reduction process is necessary for the conversion of oxides to metal. A lithium reduction process has been studied in CRIEPI for this purpose [2–5]. In these studies, not only the thermodynamic conditions necessary for reducing transuranic element oxides was elucidated, but also a MOX-pellet containing approximately 10 wt% of Pu was completely reduced to metal by incremental addition of lithium reductant to a lithium chloride melt at about 923 K, in which the MOX-pellet was immersed. The following concerns for the lithium reduction process were also pointed out in the same studies.

- (1) Lithium oxide byproducts are accumulated at the interface between reduced and non-reduced regions. Since the byproducts interfere with the direct contact between lithium reductant and MOX, the reaction rate becomes gradually slower as the reduction progresses.
- (2) The oxides of the transuranic elements, such as plutonium and americium, are not able to be reduced to metal under conditions where the concentration of lithium oxide in lithium chloride is exceeding a certain value. The limiting concentrations are determined by the difference between the Gibbs energy of formation of plutonium or americium oxides and that of lithium oxide. Furthermore, the reduction of rare-earth oxides is fairly difficult, because the limiting concentration for rare-earth reduction is very low.
- (3) Part of plutonium, americium, and some rare-earth elements can form double oxides, designated as LiMO_x ($M = \text{plutonium, americium, or rare-earth}$), which partly dissolve in the lithium chloride. Since the solubility of the double oxides increases with increasing concentration of lithium oxide in lithium chloride [3], small amounts of actinides are lost

* Corresponding author. Tel.: +81-33 480 2111; fax: +81-33 480 7956.

E-mail address: kurata@criepi.denken.or.jp (M. Kurata).

during the lithium reduction process, especially after the accumulation of lithium oxide byproducts.

Recently, Chen et al. proposed a new process for titanium oxide reduction using an electro-chemical process in molten calcium chloride salt [6]. In their process, titanium oxide can be reduced to metal by electro-chemical diffusion of oxygen ions from a titanium oxide cathode to a graphite anode through the molten salt. There are several benefits of the electro-chemical process in comparison to the lithium reduction process. Those are as follows:

- (1) As the oxygen ions in molten salt are kept at almost fixed concentration during the electro-chemical process, the thermodynamic potential is stable, thus maintaining a homogeneous product.
- (2) As the oxygen concentration in molten salt can be kept far lower in the electro-chemical process than the chemical reduction processes, it is possible to reduce not only the oxides of minor actinides but also those of rare-earths to metal [5].
- (3) Even in the case that the byproducts, such as lithium oxide, are formed at the interface between the reduced and non-reduced regions, the byproducts can be decomposed to lithium cations and oxygen anions in the electro-chemical reduction process, and then the lithium cations can be simultaneously reduced to metal so that behave as reductant.

Karell and Gourishankar applied this electro-chemical process for the direct reduction of spent oxide fuel using lithium chloride molten salt [7]. They demonstrated the reduction of small particles of uranium oxide in their study. CRIEPI has also been developing an electro-chemical reduction process applied to MOX fuel reduction, the results of which are summarized in this paper.

2. Experimental

2.1. Sample and reagent

A MOX fuel pellet, in which the concentration of Pu is $\text{Pu}/(\text{Pu} + \text{U}) = 9.45 \text{ wt}\%$, was broken into several pieces of 1–2 mm in thickness and 3–4 mm² in cross-section. The weight of these pieces was approximately 200 mg. Two pieces were used for the present test. LiCl with 99.9% purity was used as a reagent. To seed the oxygen potential during the electro-chemical reduction, a small amount of Li₂O with 99.9% purity was added to LiCl. The mixture of 60 g of LiCl and 600 mg of Li₂O was introduced in an MgO crucible and then melted at around 923 K.

2.2. Apparatus

Fig. 1 shows a schematic diagram of the test apparatus. A MgO crucible (50 mm inner diameter and 50 mm height) containing the LiCl–Li₂O mixture was set in a reactor. A glassy-carbon anode (4 mm outer diameter and 80 mm length), a MOX cathode, and a Ta-wire were introduced into the molten salt. The Ta-wire was used as a quasi-reference electrode. The glassy-carbon rod was then connected to a Ta-wire (0.5 mm diameter). The Ta-wire was covered with an Al₂O₃ tube (1 mm inner diameter) for insulation. To avoid an agitation of the molten salt by gas generated on the anode surface by the electro-chemical reaction and to avoid the migration of oxygen gas to cathode, an Al₂O₃ shroud for the immersed part of the glassy carbon anode (10 mm inner diameter and 60 mm length) was connected to the Al₂O₃ tube (see Fig. 1). A piece of MOX was placed in the basket made of two pieces of Ta-mesh (200 mesh, 8 mm × 8 mm) and a piece of Mo-mesh (500 mesh, 8 mm × 8 mm). The Mo-mesh was sandwiched between the Ta-meshes to avoid the direct contact of Mo with the reduced Pu–U alloy. A Ta-wire (1 mm diameter) with an Al₂O₃ cover as insulator was used as an electrical lead of the MOX cathode. Another Ta-wire with an Al₂O₃ cover was used as a pseudo-reference electrode during galvanostatic electro-chemical reduction of MOX. In the cyclic-voltammetry studies performed separately, Bi-30 mol%Li liquid alloy set in an MgO tube was used as a reference electrode, because the Ta quasi-reference electrode was not stable enough for the cyclic-voltammetry. All operations were performed in an Ar-atmosphere glove box in which oxygen impurity and moisture levels were maintained at lower than 10 ppm.

2.3. Procedure

After melting of the LiCl–Li₂O mixture, the cathode, anode and reference electrodes were lowered into the

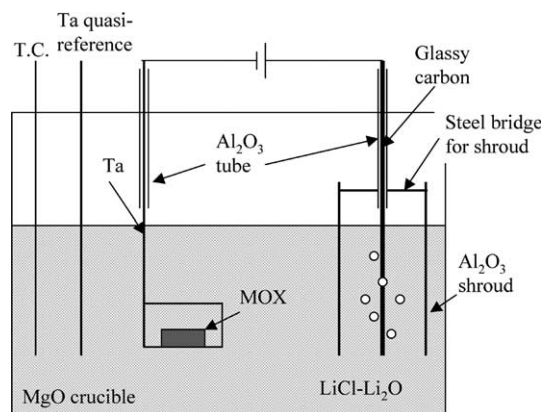


Fig. 1. Image for electro-chemical cell.

molten salt. The difference between the cathode and anode potentials was monitored during the electro-chemical reduction and maintained below 2.8 V, that was selected in the present study as the value far below the potential for LiCl decomposition at 923 K (3.46 V). The electro-chemical reduction was performed in a galvanostatic mode that corresponded to current density of approximately 50 mA/cm².

In the electro-chemical reduction of the present system, two kinds of electro-chemical reaction can possibly occur at the cathode.



The distinction of these two reactions is very difficult only from observation of the reduced material, because lithium metal formed by Eq. (2) reduces MO_x in a secondary step. In the galvanostatic mode, the above two reactions may occur simultaneously although the ratio between the reactions differs according to the electro-chemical potential conditions. In the present study, therefore, a relaxation step of approximately 30 min was introduced after each electro-chemical reduction step also of approximately 30 min. The combination of an electro-chemical reduction and a relaxation was applied several times. The electro-chemical reduction was finished when the applied current attained was 1.2 times as much as that theoretically required for the complete reduction of the MOX sample. After the electro-chemical reduction, the samples were washed with alcohol to remove salt, put into resin, and cut into two parts. Then, the polished cross-section of the samples was analyzed by means of metallography, EPMA, and SEM-EDX. In the second test, a UO₂ particle with approximately the same weight as the MOX particle was added to the cathode and the electro-chemical reduction was performed in the same manner. In the second test, therefore, the electro-chemical reduction progressed to an intermediate step.

3. Results and discussion

3.1. Structure of reduced MOX

Fig. 2 shows a secondary electron image (SEI) of a MOX cross-section after the reduction in the first test. Since the reduced sample was very brittle and porous, thorough polishing could not be carried out. Grey parts seen in Fig. 2, therefore, correspond to remaining resin on the sample surface. A coral-like structure is observed in the whole sample, suggesting that MOX was reduced completely in the first test. The formation of the coral-like structure is discussed later.

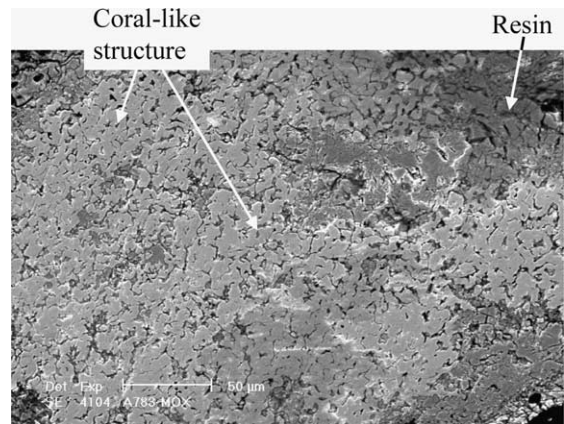


Fig. 2. SEI of cross-section of MOX reduced completely in the first test.

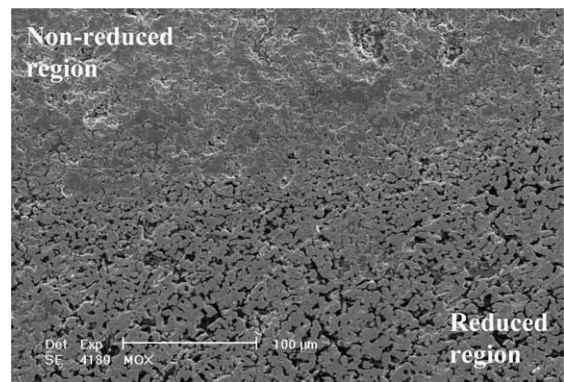


Fig. 3. SEI of cross-section of MOX reduced in the second test (around interface between reduced and non-reduced regions).

Fig. 3 shows a SEI of a MOX cross-section after the reduction in the second test, in which the reduction of MOX is not expected to be complete due to the presence of UO₂. The reaction is considered to progress from bottom to top in Fig. 3. Hereafter, the lower half and the higher half regions in Fig. 3 are named as reduced and non-reduced regions, respectively, for convenience. The coral-like structure is observed only in the reduced region, and is similar to that observed in Fig. 2. The non-reduced region appears to be denser than the reduced region.

Fig. 4 shows a metallograph of interface between the reduced and non-reduced regions of the sample. The position given in Fig. 4 is adjacent to that in Fig. 3. The coral-like structure with metallic luster apparently observed in the reduced region is similar to that seen in Fig. 3. In the non-reduced region, however, the initial stage of reduction at the grain boundaries is only observed. A network of reduced part corresponds to the

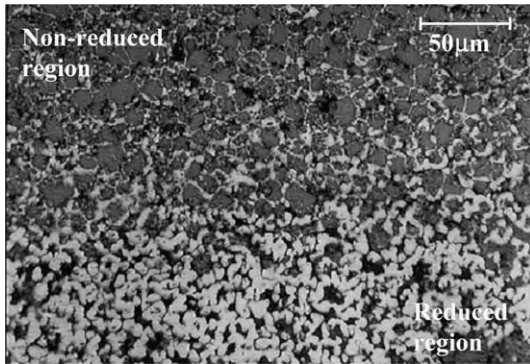


Fig. 4. Metallography of MOX cross-section reduced in the second test.

grain-boundaries of the original MOX sample. The thickness of the reduced zone around the grains decreases with distance from the reduced/non-reduced interface. These observations suggest that the grain-boundary was reduced prior to grain bulk in the non-reduced region. It is well known that the diffusion rate along a grain-boundary is in most cases far faster than that in a grain bulk. In case of the electro-chemical reduction, the reduction of the grain-boundary occurs as the first step, and thus it forms the network structure. Then, the grain bulk is reduced as the second step and the reduced alloy develops on the network structure to form a coral-like structure. The volume of the reduced product is necessarily smaller than that of the original MOX, and it would well explain why the structure of the reduced region is porous and coral-like.

Since the MOX grains are covered by the network structure of alloy in the first step, the reduction reac-

tion is afterwards controlled by the diffusion rate of oxygen ions through the network structure and is thus slower. If molten salt invades the non-reduced region by the increase in the shrinking grains, the decrease in the reaction rate might be counterbalanced by the increase in the reaction surface. The morphology of the initial material will therefore significantly affect the reaction rate.

3.2. Distribution of Pu and U in reduced product

Fig. 5(a) indicates an absorption electron image at the interface between the reduced and non-reduced regions. Fig. 5(b) and (c) show U- and Pu-map for the same position. The reduction reaction progresses from left to right in the figures. The white color in the X-ray maps indicates the density of each element. U exists mostly homogeneously in the coral-like structure in the reduced region and the U-density in the reduced region is obviously higher than that in the non-reduced region where U mostly exists as oxide. Regarding to Pu, fine Pu-spots are observed in the reduced region. Comparing Fig. 5(c) to Fig. 5(a) and (b), Pu-spots seem to exist outside the coral-like structure. Inside coral-like structure, however, Pu exists rather homogeneously and the density of Pu appears lower than that in the original MOX. Quantitative point analysis was performed for several points in the reduced and non-reduced regions using EPMA. The results indicate that the Pu-concentration in the coral-like structure varies from 3 to 5 wt%. These values are clearly smaller than that of the original MOX sample (9.45 wt%).

In the reduced/non-reduced interface region, on the other hand, Pu condenses on the surface of non-reduced

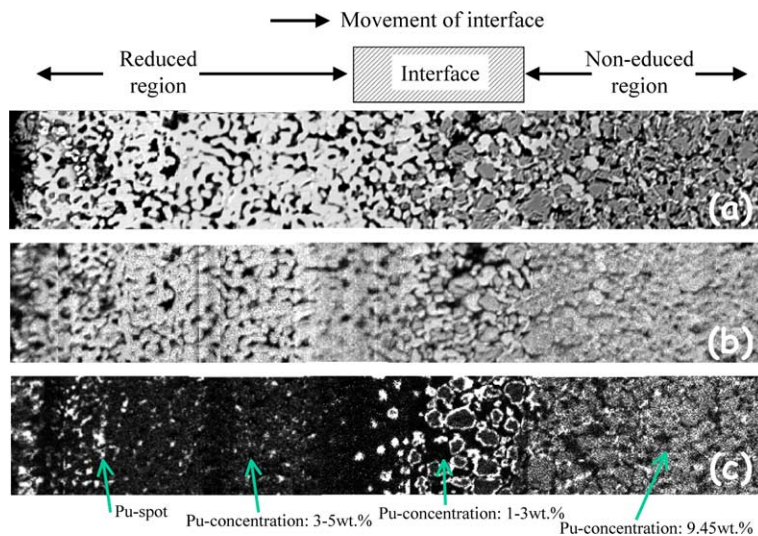


Fig. 5. Absorption electron image and U- and Pu-maps of interface between reduced and non-reduced region. (a) Absorption electron image, (b) U-map and (c) Pu-map.

MOX grains. As the thickness of the Pu-condensed layer is too thin for the quantitative point analysis, the Pu-concentration of the layer could not be measured. The point analysis was only performed for the reduced parts adjacent to the Pu-condensed layer. The Pu-concentration in those parts varies from 1 to 3 wt%. These values are not only obviously smaller than that of the original MOX but also the average value for the coral-like structure in the reduced region. These facts suggest that the reduction rate of U is faster than that of Pu, and that Pu is pushed out of the firstly reduced part and precipitates on the surface of MOX grains. Then, Pu begins to be reduced and might be dissolved again in the coral-like structure. Small amount of Pu precipitates out of the coral-like structure in the same time. For the further discussion, an accurate analysis on the oxygen distribution is being planned to confirm whether those Pu-condensed spot and layer are oxide or metal.

According to the Pu–U phase diagram, the solubility of Pu in U at 923 K is approximately 5 wt%. This value almost coincides with the Pu-concentration in the coral-like structure, which was detected in the present study. This might be an upper-limit of the Pu-concentration for the alloys, in which Pu and U homogeneously exist. After the experiment, small amount of Pu-rich powder was detected in the salt collected from the bottom of the MgO crucible. Since the reduction of U occurred prior to that of Pu, small amount of Pu was thought to be dropped off from the sample. It is however important to keep Pu retained inside of the cathode, when applying the electro-chemical process on an industrial scale.

3.3. Reduction and relaxation

Fig. 6 shows the variation in the potential between the cathode and anode for each cycle of the reduction and relaxation in the first test. In the cycles 1 and 2, the potential between cathode and anode is maintained between 1.4 and 2.0 V until the electro-chemical reduction is attained approximately after 12 min. Then, it increases gradually to between 2.1 and 2.2 V. In the same time, the

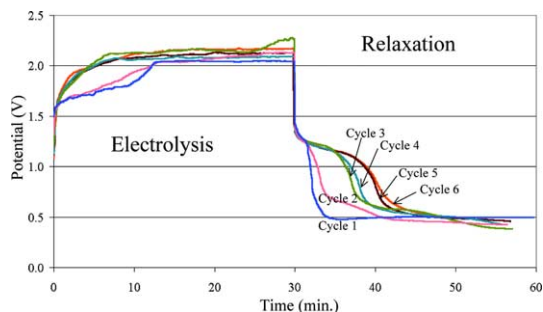


Fig. 6. Variation in potential between glassy carbon anode and MOX cathode during electrolysis and relaxation.

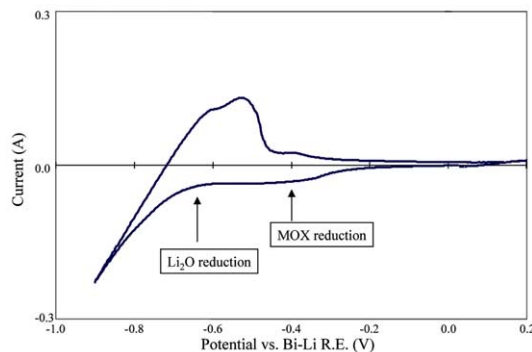


Fig. 7. Cyclic-voltammogram for electro-chemical reduction of MOX in LiCl-1wt%Li₂O (923 K).

anode potential was kept stable. In the other cycles, this kind of variation is not observed. This fact is explained as follows. Fig. 7 shows a typical cyclic-voltammogram for MOX reduction. The reduction for Li₂O and MOX are marked in the figure and the difference between these reductions is approximately 0.2–0.3 V. This difference almost coincides to the change in the potential observed in the cycles 1 and 2 of the first reduction test. This suggests that the direct reduction of MOX plays a major role in the beginning of the electro-chemical reduction, and then later the indirect reduction of Li-oxide, becomes significant. The network structure of the reduced alloy (as seen in Fig. 4) might form on the surface of the MOX sample after cycle 3, and it seems likely to interfere with the direct electro-chemical reduction.

Regarding the potential variation in the relaxation step, it rapidly attains the rest potential in cycles 1 and 2, but an intermediate step appears between the imposed and rest potentials after cycle 3 at about 1.3 V. The reason for this variation is not clear, but probably it corresponds to the dissolution of Li deposit from the MOX surface by the melt or the disappearance of Li deposit due to chemical reaction with the MOX.

4. Summary

A piece of MOX weighing a few hundreds of milligrams were completely reduced to metal by electro-chemical process. The direct electro-chemical reduction of the UO₂ or PuO₂ played a major role in the beginning and, thereafter, indirect reduction became significant. This process appears to initiate at the grain boundaries of the MOX before slowly penetrating into the grain bulk. This phenomenon caused a formation of the coral-like structure for the reduced metallic product. The Pu-concentration in the coral-like structure of the reduced product was approximately 3–5 wt%, which was smaller than that in the original MOX (9.45 wt%) and

almost coincided with the Pu-solubility reported for the Pu–U alloy at 923 K. The rest of the Pu formed Pu-rich spots outside the coral-like structure. They were probably the original centers of the MOX. These phenomena suggest that the development of cathode container is very important to the electro-chemical process.

Acknowledgements

The authors are indebted to Drs Malmbeck and Somers for preparation of MOX samples. The authors would like to appreciate to Drs Walker, Wiss, and Murray-Farthing for their great help on EPMA, SEM-EDX, and metallography. Also, the authors would like to thank Drs Bottomley, Sakamura, and Iizuka for useful discussion on electro-chemistry.

References

- [1] T. Inoue, H. Tanaka, in: Proceedings of International Conference on Future Nuclear Systems (GLOBAL), 1997, p. 646.
- [2] T. Usami, M. Kurata, T. Inoue, H.E. Sims, S.A. Beetham, J.A. Jenkins, *J. Nucl. Mater.* 300 (2002) 15.
- [3] T. Usami, T. Kato, M. Kurata, T. Inoue, H.E. Sims, S.A. Beetham, J.A. Jenkins, *J. Nucl. Sci. Technol.* 3 (supplement) (2002) 858.
- [4] T. Usami, T. Kato, M. Kurata, T. Inoue, H.E. Sims, S.A. Beetham, J.A. Jenkins, *J. Nucl. Mater.* 304 (2002) 50.
- [5] M. Kurata, R. Yuda, T. Kato, T. Usami, *J. Nucl. Mater.*, in press.
- [6] G.Z. Chen, D.J. Fray, T.W. Farthing, *Nature* 407 (2000) 361.
- [7] E.J. Karell, K.V. Gourishankar, in: Proceeding of the American Nuclear Society Topical Meeting on DOE Spent Nuclear Fuel and Fissile Material Management, Charleston, SC, September 1998.